5ICEGE
5th International Conference on Earthquake Geotechnical Engineering
January 2011, 10-13 | Santiago, Chile
Paper No. MLSME

MONITORING LARGE-SCALE SHAKING TABLE TEST USING VIDEO RECORDING AND MOTION TRACKING ANALYSIS

Claudia MEDINA[1], Ricardo DOBRY[2], Mourad ZEGHAL[3], Sabanayagam THEVANAYAGAM[4], Tarek ABDOUN[5], Ahmed ELGAMAL[6], Usama EL SHAMY[7], Victoria BENNETT[8]

ABSTRACT

This paper presents an innovative development of the use of video camera recordings in conjunction with a motion tracking software to provide a complete set of soil lateral displacement recordings as a function of depth and time during shaking-induced lateral spreading in a full-scale test. The test was conducted at the University of Buffalo 1g shaking table as part of an NSF's George E. Brown, Jr., Network for Earthquake Engineering Simulation (NEES) collaboration project. A soil model having a 6-m height was tested in a laminar box inclined 2 degrees to simulate a mild infinite slope with a saturated uniform fine sand layer. The model was subjected to a base shaking that induced liquefaction and lateral spreading. The 1g testing involved the use of extensive and state-of-the-art instrumentation techniques to measure the soil response and the innovative use of motion tracking analysis from one of the video camera records. The instrumentation was aimed at recording the dynamic response as well as permanent changes in the free field. Cross-comparisons of data records showed outstanding agreement between different instrumentation technologies, and the systematic use of the video camera recording allows the development of a complete picture of the lateral displacement response of the deposit with an unprecedented degree of resolution in time and space. The motion tracking analysis from the video taken by the North Video Camera provided additional lateral displacement information that proved essential for a more complete analysis and interpretation of the full-scale test results.

Keywords: Motion tracking analysis, full-scale test, lateral spreading, liquefaction.

INTRODUCTION

In recent years, digital image sequences have become an increasingly common and important component in technical and engineering applications, ranging from medical imaging and multimedia communications to use in autonomous vehicle navigation and physical testing. Video analysis has shown great potential applications in a large number of different areas such as: crash tests in automotive industry, tracking of fluid object development, military test ranges, medicine and heath industry, and coaching system helping athletes to improve performance.

---

[1] Geotechnical Engineer, BGC Engineering Inc., Vancouver, BC, Canada, e-mail: cmedina@bgcengineering.ca
[2] Professor, Department of Civil & Environmental Engineering, Rensselaer Polytechnic Institute, Troy, NY, USA.
[3] Associate Professor, Department of Civil & Environ. Eng., Rensselaer Polytechnic Institute, Troy, NY, USA.
[4] Associate Professor, Dept. of Civil, Struct. & Environ. Eng., University at Buffalo SUNY, Buffalo, NY, USA.
[5] Associate Professor, Department of Civil & Environ. Eng., Rensselaer Polytechnic Institute, Troy, NY, USA.
[6] Professor, Department of Structural Engineering, University of California San Diego, La Jolla, CA, USA.
[7] Associate Professor, Department of Civil & Environ. Eng., Southern Methodist University, Dallas, TX, USA.
[8] Ph.D. Student, Dept. of Civil & Environ. Eng., Rensselaer Polytechnic Institute, Troy, NY, USA.

Digital image sequences are used to track objects in images and make analysis of the movement. The commercial software TrackEye Motion Analysis (TEMA) was used in the work reported here in to analyze and track the movement of the full-scale test aimed to investigate the mechanism of shaking-induced lateral spreading.

Lateral spreading due to liquefaction of saturated cohesionless soils is a common and extremely damaging phenomenon to deep foundations occurring during earthquakes. It typically happens near waterfronts or in mildly sloping areas, with permanent lateral displacements of the ground ranging from a few centimeters to several meters (Dobry and Abdoun, 2001). A first and very important step when addressing liquefaction-induced lateral spreading of sloping ground is to fully understand the response of the lateral displacement response of the free field. Despite the extensive research efforts on the last 20 to 30 years (e.g., Ashford et al., 2006; Suzuki et al., 2005; Tamura and Tokimatsu, 2005; Towhata et al., 2006; He et al., 2006; Abdoun et al., 2003; Haig and Madabhushi, 2005; Brandenberg et al., 2005, 2007), the mechanics of lateral spreading in the free field remains poorly understood and the most reliable engineering methods for predicting lateral ground deformation remain empirical correlations or simplified analyses calibrated with case histories (e.g., Youd et al., 2002; Olson and Johnson, 2008).

An extensive and cooperative research aimed at detailed clarification and quantification of the mechanics of soil-pile interaction during lateral spreading, is been carried out by four US universities with the support of the US National Science Foundation through the NEES Consortium, NEES Inc. (NEES: George E. Brown, Jr. Network for Earthquake Engineering Simulation). The centerpiece of the effort is the 1g full scale testing in the 6-m tall laminar box recently developed at University of Buffalo, shown in Figure 1(a). Two successful sand liquefaction free field experiments have already been conducted using this laminar box: (i) Test LG-0, with the laminar box placed horizontally simulating liquefaction of a level deposit; and (ii) Test SG-1, with the laminar box inclined 2 degrees to the horizontal to simulate liquefaction and lateral spreading of a mildly sloping deposit. A full description of these tests is reported by Bethapudi (2008) and Thevanayagam et al. (2003, 2009).

This paper presents an innovative development and use of video camera recordings in conjunction with tracking software, to provide a complete set of soil lateral displacement recordings during shaking-induced lateral spreading in the full-scale shaking table Test SG-1. The technique produced lateral displacements time histories, D_H, for all laminar box rings on the shaking table with an unprecedented degree of resolution in time and space, allowing the development of a complete picture of the lateral displacement and strain response of the deposit. A complete analysis and discussion of the mechanics of lateral spreading observed in this test are presented by Dobry et al. (2010).

DESCRIPTION OF FULL-SCALE SHAKE TEST

The full-scale test conducted at the University of Buffalo 1g shaking table, named Test SG-1, involved a 5.57m deep, loose saturated sand deposit constructed inside the laminar box shown in Figure 1(a). The relative density of the deposit of the sand varied between 30 to 50% (void ratio ranging between 0.7-0.75), with an average value of 40%. Additional data on this sand including laboratory index properties, stress-strain testing results, as well as field measurements inside the laminar box of the hydraulically deposited sand are presented by Thevanayagam et al. (2003, 2009) and Bethapudi (2008). The laminar box used in Test SG-1 consists of a stack of 24 identical, 25.4cm high aluminum rings (laminates L1 to L24) separated by spherical ball bearing units allowing a maximum relative lateral interlaminate displacement of 36 mm. The center-to-center distance between adjacent laminates is 25.9 cm. The bottom ring (L1) was tied to the shaking base and the top three rings L22, L23 and L24 were tied together. Each laminate above L1 was inclined to slide along the ball bearing units at 2 degrees with respect to the horizontal in the longitudinal direction, as shown in Figures 1(a) and 1(b), to simulate an infinitely long gently sloping ground in the field. In this test, the soil was filled up to the mid-level of L22, so the total depth of sand that could move freely in a lateral direction was 5.32m, corresponding to the total depth of sand (5.57m) minus the height of bottom ring L1 (0.25m).

A dense instrumentation array was setup inside the soil and on the laminates to measure the response of the soil during the experiment. This instrumentation array consisted of accelerometers, pore pressure transducers, potentiometers measuring lateral displacements and settlements, and two state-of-the-art MEMS ShapeAccelArrays-SAA measuring both horizontal accelerations and displacements at 30cm intervals within the soil (Bennett et al., 2007 and Abdoun et al., 2008). Four video cameras were also installed in key locations to capture the motion of the laminar box in different directions.

The layout of the mentioned instruments is shown in Figure 1(b). A detailed description of the entire test setup is presented in Thevanayagam et al. (2008). The input base motion as described in Figure 1(c) was applied at the base in the longitudinal direction by actuators connected to a strong wall. This input accelerogram had a duration of 8.4s and a frequency of 2Hz, consisting of a total of about 17 sinusoidal cycles. The base motion consisted of 5s of a sinusoidal motion at amplitude of 0.01g, termed the non-destructive shaking (NDS). After the NDS, the amplitude was stepped up to 0.05g with a small transition consisting of 2 cycles, phase that was designed to liquefy the deposit and induce significant permanent displacement in the downslope direction, as presented in Dobry et al. (2010).

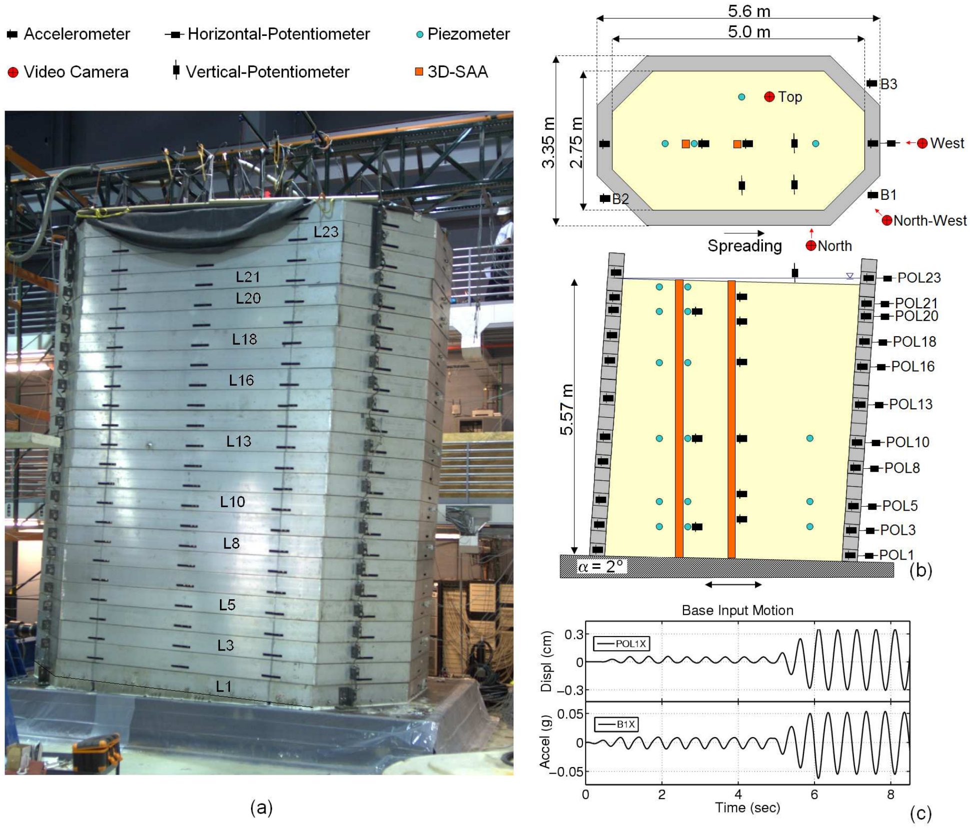

Figure 1. Laminar Box. (a) Picture of SG1 test before shaking; (b) Setup and instrumentation of SG1 test; and (c) Input displacement and acceleration base motion.

DESCRIPTION OF VIDEO MOTION TRACKING ANALYSIS TECHNIQUE

As mentioned before, Test SG-1 involved the use of state-of-the-art instrumentation techniques, including four video cameras installed in key locations to capture the motion of the laminar box (Fig. 1(b)). The lateral displacement of the laminar box was recorded by a camera installed perpendicular to the longitudinal direction (E-W) pointing from the North (referred as North Video Camera). The sequences of images from the North Video Camera were digitalized and used to track target points at each ring and produce lateral displacement time histories for all laminar box rings, additional information that proved essential for a more complete analysis and interpretation of the full-scale test results.

The commercial software TEMA was used to analyze the video sequence. A number of different tracking algorithms are available in this software, and tracking of several points through the image sequence is also allowed. The 2D-tracking is the basic functionality of TEMA and it was used to analyze and track the motion of the targets points. This tracking function operates in two dimensions and produces 2D pixel coordinates for each tracked point in each image, generating output plots with relative displacement between the tracked points (Photo-Sonics, Inc., 2009). Figure 2 shows four digitalized images (snapshots) from the North Video Camera at 0, 5, 6 and 8.4 seconds of shaking. The snapshots show the permanent displacement and the schematic targets points for each ring used in the motion tracking analysis.

Plots of relative lateral displacement between rings were generated using this software. Absolute lateral displacements were measured during the test using two different type of sensors: (i) horizontal potentiometers mounted on the eleven laminates of the laminar box which are labeled L1, L3, L5, L8, L10, L13, L16, L18, L20, L21 and L23 in Figure 1(a); and (ii) horizontal displacement sensors included in the two vertical SAA arrays placed within the soil as shown in Figure 1(b).

Due to the fact that the vertical SAA arrays were used for the first time in this type of tests, the data recorded by the potentiometer sensors sicwas considered more reliable measurements of the actual lateral displacements and, they were used as basic reference to generate the corresponding absolute lateral displacement time history of each ring. An automatic optimization procedure embedded in the Matlab software was used to match the data recorded by the potentiometers located in some of the rings and the data obtained from the video motion analysis.

SUMMARY AND DISCUSSIONS OF VIDEO MOTION TRACKING RESULTS

Figure 3 shows the comparison between the total lateral displacement (i.e., cyclic and permanent (noncyclic) component) time histories curves obtained from both potentiometer records and the record generated by the motion tracking video analysis. In this figure, positive displacement indicates downslope motion and negative displacement indicates upstream motion. Note that the curve of the bottommost laminate (z=5.45m) is the same as the input motion (Figure 1(c)), since this laminate was attached to the shaking floor. This figure shows excellent agreement between the lateral displacement recorded by the potentiometer and the lateral displacement estimated using the motion tracking software and optimization procedure.

Time histories of the total lateral displacement for each one of the 22 laminate obtained with this procedure are shown in Figure 4. Note that laminates L22, L23 and L24 were tied together and therefore they move together.

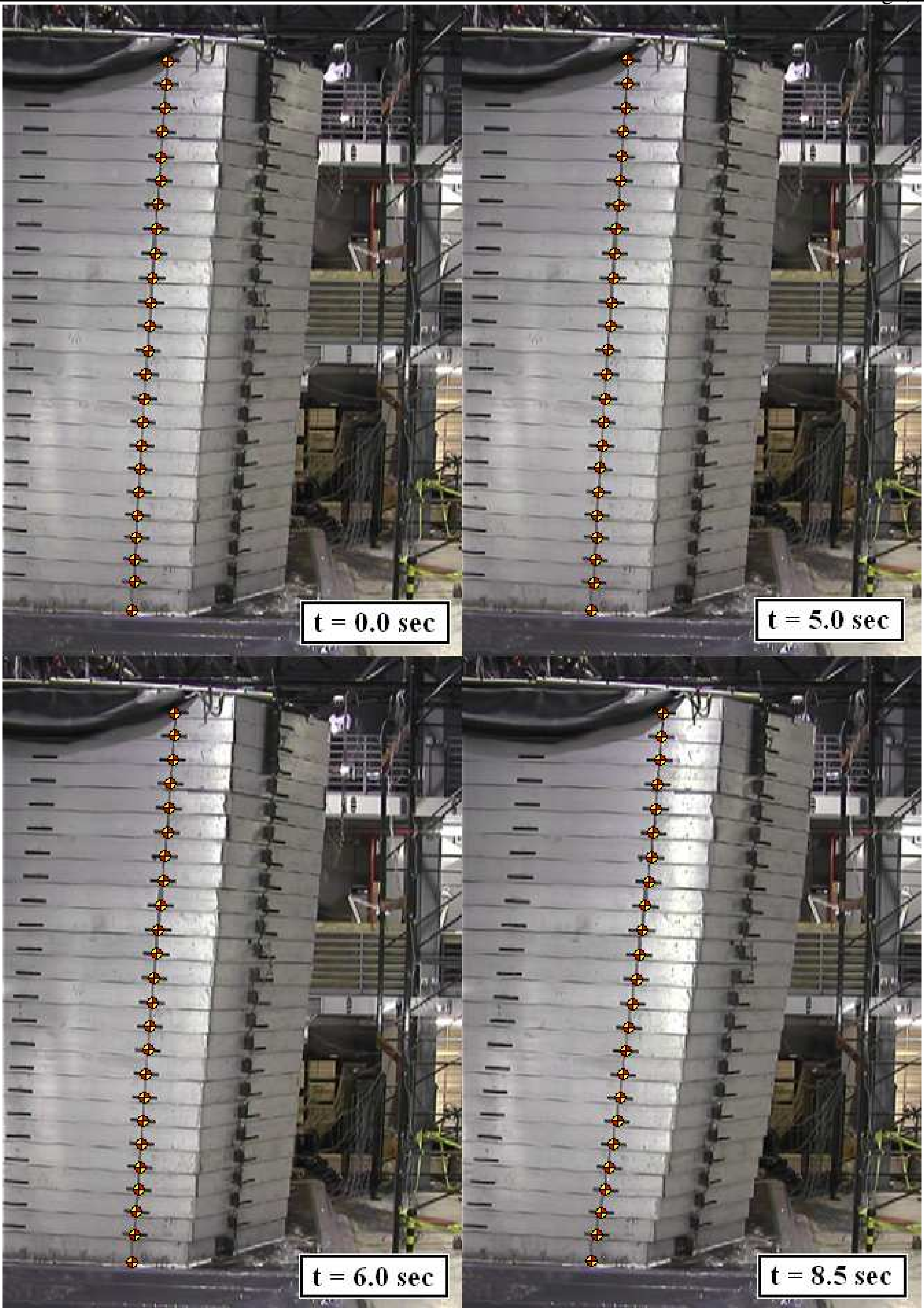

Figure 2. Frames from north camera video showing permanent displacement and schematic target used for the video motion analysis.

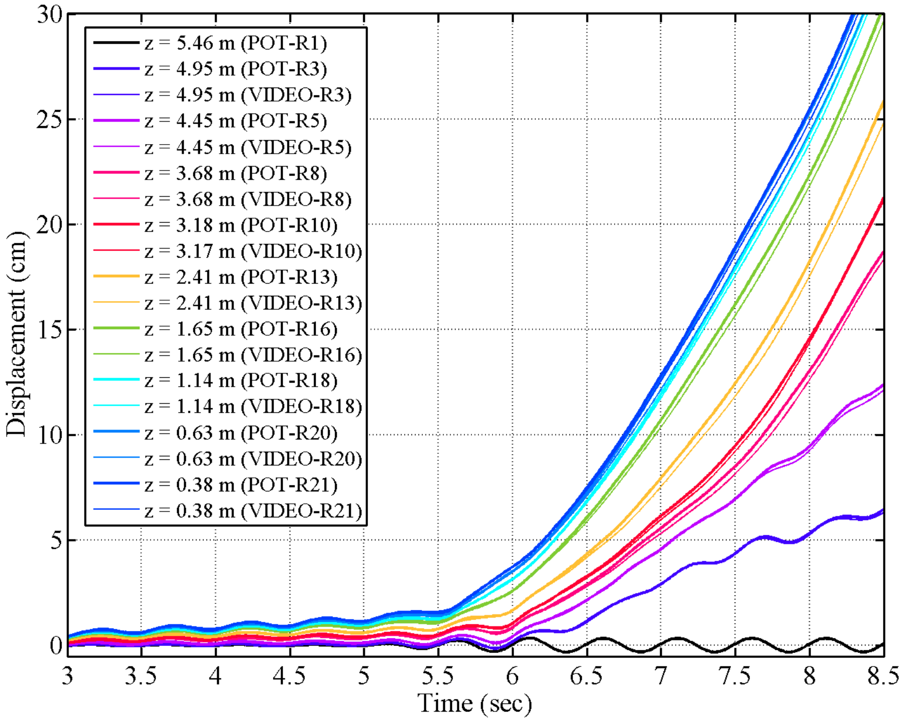

Figure 3. Time history of total lateral displacement at certain locations. Comparison between curves obtained between potentiometer records and video motion analysis records.

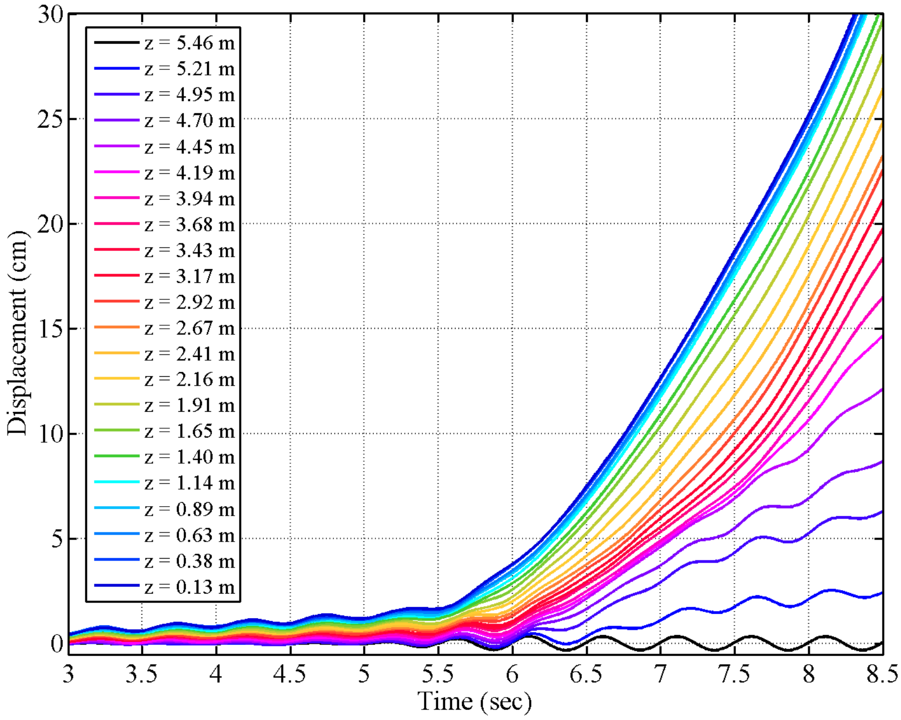

Figure 4. Time history of total lateral displacement for each laminate. Curves obtained from video motion analysis for each ring.

The permanent (noncyclic) lateral displacement profiles for the time frame between 5 and 8.4s at 0.5s intervals are presented in Figure 5(a). The permanent lateral displacement plot was obtained by filtering the frequencies above 1Hz. This figure shows the data obtained with different instrumentation including: potentiometers attached to the laminates, video motion analysis of each laminate and the SAA array within the soil deposit. There is excellent agreement between the different types of instrumentation. A solid line, evaluated as the best curve fitting, was added to show the global trend of the permanent lateral displacement of the soil layer in test SG-1.

Permanent (noncyclic) velocity profiles obtained by time-differentiating the permanent lateral displacement (filtered above 1Hz) are presented in Figure 5(b) for the different instrument types. This figure shows the global velocity trend of the soil deposit during the Test SG-1. Good agreement between different instrumentation is also achieved for these permanent velocity records. The SAA data, however, shows some disagreement at the end of the shaking (t>8s). Note that this type of instrument was not designed to record cyclic lateral displacements, thus the slight differences in the SAA data observed in Figure 5(a) is further increased by the time-differentiation used to obtain the results in Figure 5(b). Similarly to the lateral displacement profiles, the solid lines show the global trend of the permanent lateral velocity of the soil deposit in Test SG-1. These curves were obtained by time-differentiating the solid lines representing the permanent lateral displacement profiles of the soil deposit in Figure 5(a).

As mentioned previously, Test SG-1 was conducted in the inclined laminar box in an attempt to approximate the spreading of an infinite slope. The shearing planes lied between the adjacent laminates, and were parallel to the sloping angle of 2 degrees. Figure 5(c) presents the permanent shear strain (γ_p) profiles. These curves were obtained by differentiating with respect to depth the solid lines representing the permanent lateral displacement profiles of the soil deposit (Figure 5(a)). This Figure5 (c), made possible only due to the availability of the lateral displacement records generated by the video motion analysis, proved to be a key piece of information for the analysis and interpretation of the shaking-induced lateral spreading initiation and soil response as discussed in detail by Dobry et al., 2010.

CONCLUSIONS

Motion tracking analysis from the video taken by the North Video Camera provided additional lateral displacement information that proved essential for a more complete analysis and interpretation of Test SG-1.

The North Video Camera data gives a complete picture in two critical respects: (i) it provides time histories of lateral displacement for all 22 laminar box rings of interest (compared with the discontinuous information from potentiometers on eleven rings, see Figures 1 and 3); and (ii) it naturally includes both the cyclic and non-cyclic (permanent) components of the lateral displacement, as illustrated by Figures 4 and 5 (compared with information for only the non-cyclic component provided by the SAA sensors).

The lateral displacement information obtained from the three set of sensors is completely consistent. The systematic use of the North Video Camera recordings provides a complete picture of the lateral displacement response of the deposit that can be used with a high degree of confidence.

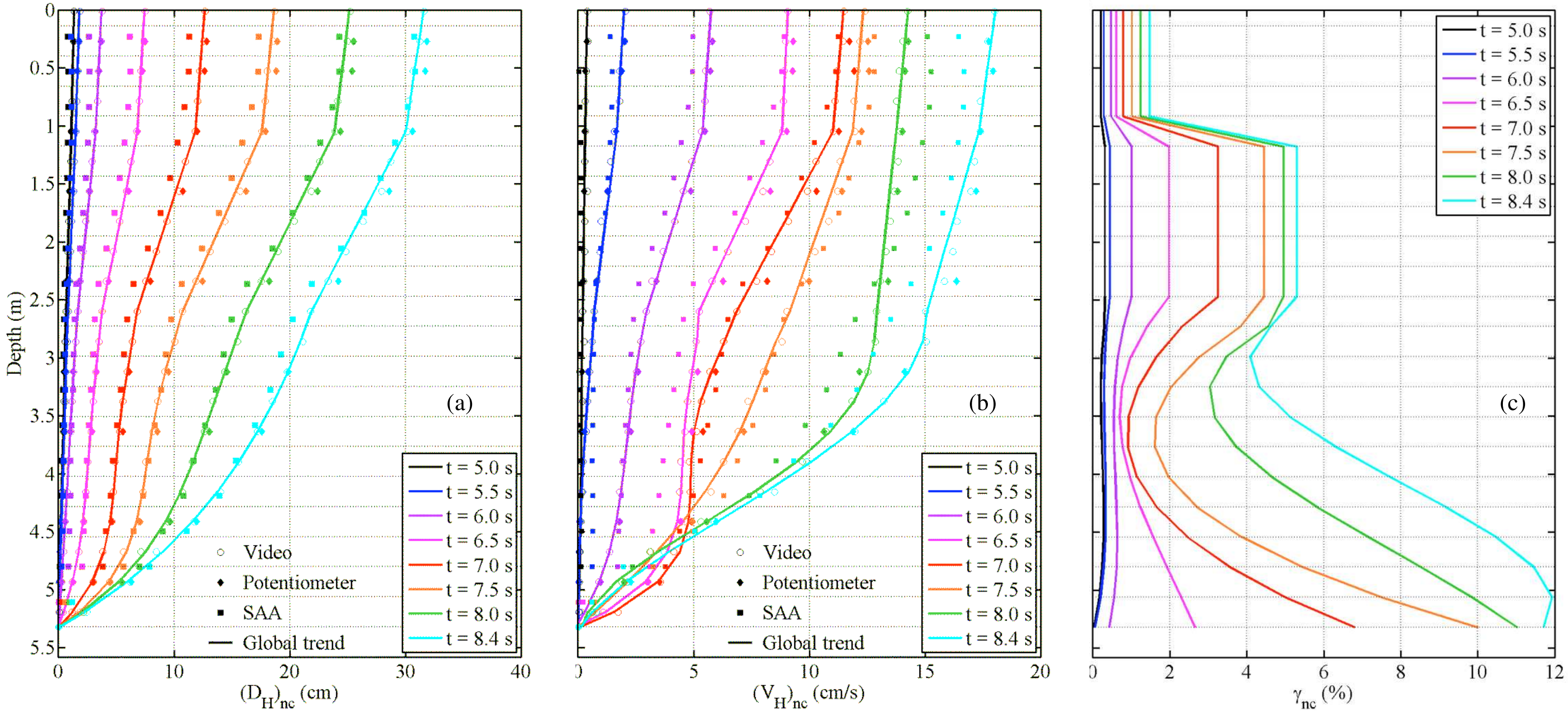

Figure 5. Profiles of key parameters measured during strong shaking in Test SG-1, after removing the cyclic component (filtered above 1Hz): (a) permanent (noncyclic) lateral displacement – best fitting curve (solid lines), data from North Video Camera (circles), data from potentiometers (diamonds), and data from SAA array (squares); (b) permanent (noncyclic) velocity - best fitting curve (solid lines), data from North Video Camera (circles), data from potentiometers (diamonds), and data from SAA array (squares); (c) permanent (noncyclic) shear strain.

AKNOWLEDGEMENTS

This material is based upon work supported by the National Science Foundation under NEESR-SG Grant No. 0529995. This support is gratefully acknowledged.

REFERENCES

Abdoun, T., Dobry, R., O'Rourke, T. D., and Goh, S. H. (2003). "Pile Response to Lateral Spreads: Centrifuge Modeling." J. Geotech. Geoenviron. Eng., 129(10), 869-878.

Abdoun, T., Bennett, V., Dobry, R., Thevanayagam, S., and Danisch, L. (2008). "Full-Scale Laboratory Tests Using a Shape-Acceleration Array System." Proc. of the 4th decennial Geotechnical Earthquake Engineering and Soil Dynamics Conference (GSP 181). Sacramento, CA, May 18-22.

Ashford, S.A., Juirnarongrit, T., Sugano, T., and Hamada, M. (2006). "Soil-Pile Response to Blast-Induced Lateral Spreading. I: Field Test," J Geotech Geoenviron Eng, Vol. 132, No. 2, pp. 152-162.

Bennett, V., Zeghal, M., Abdoun, T., and Danisch, L. (2007). "A Wireless Shape-Acceleration Array System for Local Identification of Soil and Soil-Structure Systems." Transportation Research Record: Journal of the Transportation Research Board, Soil Mechanics 2007, No. 2004, pp. 60-66.

Bethapudi, R. (2008). "Liquefaction Induced Lateral Spreading in Large-Scale Shake Testing." M. S. Thesis, Dept. of Civil, Structural and Environmental Engineering, University at Buffalo, Buffalo, NY, August.

Brandenberg, S.J., Boulanger, R.W., Kutter, B.L., and Chang, D. (2005). "Behavior of Pile Foundations in Laterally Spreading Ground During Centrifuge Tests," J Geotech Geoenviron Eng, Vol. 131, No. 11, pp. 1378-1391.

Brandenberg, S.J., Boulanger, R.W., Kutter, B.L., and Chang, D. (2007). "Liquefaction-Induced Softening of Load Transfer Between Pile Groups and Laterally Spreading Crusts," J Geotech Geoenviron Eng, Vol. 133, No. 1, pp. 91-103.

Dobry, R., and Abdoun, T. (2001). "Recent Studies on Seismic Centrifuge Modeling of Liquefaction and its Effect on Deep Foundation," State-of-the-Art Paper, Proc 4th Int Conf on Recent Advances in Geotech Earthq Eng and Soil Dyn (S. Prakash, ed.), Paper SOAP 3, Vol. 2, 30 pages, San Diego,CA, March 26-31.

Dobry, R., Thevanayagam, S., Medina, C., Bethapudi, R., Elgamal, A., Bennett, V., Abdoun, T., Zeghal, M., El Shamy, U., and Mercado, V. M. (2010). "Mechanics of Lateral Spreading Observed in a Full-Scale Shake Test." J. Geotech. Geoenviron. Eng., (Accepted).

Haigh, S.K., and Madabhushi, S.P.G. (2005). "The Effect of Pile Flexibility on Pile-Loading in Lateral Spreading Slopes," ASCE GSP No. 145 (Boulanger and Tokimatsu, eds.), pp. 24-37.

He, L., Elgamal, A., Abdoun, T., Abe, A., Dobry, Meneses, J., Sato, M., and Tokimatsu, K. (2006). "Lateral Load on Piles Due to Liquefaction-Induced Lateral Spreading During 1G Shake Table Experiments," Proc., 8th U.S. National Conf on Earthq Eng, Paper No. 881, San Francisco, CA,April 18-22.

Olson, S. M., and Johnson, C. I. (2008). "Analyzing Liquefaction-Induced Lateral Spreads Using Strength Ratios." J. Geotech. Geoenviron. Eng., 134(8), 1035-1049.

Photo-Sonics, Inc. (2009). <www.photosonics.com> July 10, 2009.

Suzuki, H., Tokimatsu, K., Sato, M., and Abe, A. (2005). "Factor Affecting Horizontal Subgrade Reaction of Piles During Soil Liquefaction and Lateral Spreading," ASCE GSP No. 145 (Boulanger and Tokimatsu, eds.), pp. 1-10.

Tamura, S., and Tokimatsu, K. (2005). "Seismic Earth Pressure Acting on Embedded Footing Based on Large-Scale Shaking Table Tests," ASCE GSP No. 145 (Boulanger and Tokimatsu, eds.), pp. 83-96.

Thevanayagam, S., Shenthan, T., and Kanagalingam, T. (2003). "Role of Intergranular Contacts on Mechanisms Causing Liquefaction and Slope Failures in Silty Sands." Final Report USGS Award No. 01HQGR0032 and 99HQGR0021, US Geological Survey, Dept. of Interior, 396p.

Thevanayagam, S., Kanagalingam, T., Reinhorn, A., Tharmendhira, R., Dobry, R., Pitman, M., Abdoun, A., Elgamal, A., Zeghal, M., Ecemis, N., and El Shamy, U. (2009). "Laminar Box System for 1-g Physical Modeling of Liquefaction and Lateral Spreading," Geotechnical Testing Journal, ASTM, Vol. 32 (5) 438-449, September.

Towhata, I., Sesov, V., Motamed, R., and Gonzalez, M. (2006). "Model Tests on Lateral Earth Pressure on Large Group Pile Exerted by Horizontal Displacement of Liquefied Sandy Ground," Proc 8th U.S. National Conf on Earthq Eng, Paper No. 1227, San Francisco, CA, April 18-22.

Youd, T. L., Hansen, C. M., and Bartlett, S. F. (2002). "Revised Multilinear Regression Equations for Prediction of Lateral Spread Displacement." J. Geotech. Geoenviron. Eng., 128(12), 1007-1017.